



Article

Development of Silica Nanoparticle Supported Imprinted Polymers for Selective Lysozyme Recognition

Anika Kotyrba ¹, Mehmet Dinc ² and Boris Mizaikoff ^{1,2,*}

¹ Institute of Analytical and Bioanalytical Chemistry, Ulm University, Albert-Einstein-Allee 11, 89081 Ulm, Germany; anika.kotyrba@uni-ulm.de

² Hahn-Schickard, Ulm, Sedanstraße 14, 89077 Ulm, Germany; mehmet.dinc@hahn-schickard.de

* Correspondence: boris.mizaikoff@uni-ulm.de

Abstract: Protein imprinted MIPs show notable potential for applications in many analytical areas such as clinical analysis, medical diagnostics and environmental monitoring, but also in drug delivery scenarios. In this study, we present various modifications of two different synthesis routes to create imprinted core-shell particles serving as a synthetic recognition material for the protein hen egg white (HEW) lysozyme. HEW lysozyme is used as food additive E 1105 for preservation due to its antibacterial effects. For facilitating quality and regulatory control analysis in food matrices, it is necessary to apply suitable isolation methods as potentially provided by molecularly imprinted materials. The highest binding capacity achieved herein was 58.82 mg/g with imprinting factors ranging up to 2.74, rendering these materials exceptionally suitable for selectively isolating HEW lysozyme.

Keywords: molecularly imprinted polymers; MIP; protein imprinting; core-shell imprinting; core-shell particles; lysozyme



Citation: Kotyrba, A.; Dinc, M.; Mizaikoff, B. Development of Silica Nanoparticle Supported Imprinted Polymers for Selective Lysozyme Recognition. *Nanomaterials* **2021**, *11*, 3287. <https://doi.org/10.3390/nano11123287>

Academic Editors: Camelia Bala and Alessandra Maria Bossi

Received: 8 November 2021

Accepted: 1 December 2021

Published: 3 December 2021

Publisher's Note: MDPI stays neutral with regard to jurisdictional claims in published maps and institutional affiliations.



Copyright: © 2021 by the authors. Licensee MDPI, Basel, Switzerland. This article is an open access article distributed under the terms and conditions of the Creative Commons Attribution (CC BY) license (<https://creativecommons.org/licenses/by/4.0/>).

1. Introduction

Molecular imprinted polymers (MIPs) are crosslinked polymers with specific binding moieties for selectively binding target molecules. The interaction between the MIP and the corresponding target molecule is mimicking nature via various complementary binding processes (lock and key model), e.g., antigen-antibody, DNA-protein, ligand-receptor, and peptide-protein interaction. Therefore, imprinted polymers are expected to show a high affinity and selectivity towards the target molecule and should be able to discriminate and isolate them from closely related structures. MIPs can be prepared for a wide variety of targets, e.g., proteins, viruses, drugs or pesticides [1–4]. In contrast to natural receptors, MIPs can withstand much harsher conditions, such as high temperature, pressure, pH and organic solvents. Additionally, synthetic polymeric receptors are also less expensive to synthesize and their preparation can be easily scaled up for commercial and industrial applications [4]. The technology of molecular imprinting enables the creation of artificial binding sites within a polymer matrix. These sites are tailored in situ via co-polymerization of functional monomers and crosslinkers around the template [5,6]. Afterwards, the template molecule is extracted from the obtained polymer, leaving complementary cavities (regarding shape, size, and distribution of functional groups) within the polymeric network [1–4]. For this reason, MIPs show notable potential for applications in many analytical areas, such as clinical analysis, medical diagnostics, environmental monitoring, but more recently also for assisting drug delivery [4,7]. For example, they can be employed in high-performance liquid chromatography [8], solid phase extraction [9], sensors [10], separation [11,12], and catalysis [13,14]. However, the rebinding process depends on the diffusion of the template on the recognition sites. Therefore, small molecules are easier to imprint than macromolecules or entire biological species (i.e., peptides, proteins, DNA, viruses and bacteria), which can be limited by size, mass transfer, conformational instability, etc. [15] Specifically, mass transfer to and through the crosslinked polymer matrix is

limited due to the molecular weight, which limits template removal and fast rebinding, which also results in a low binding capacity [15–17]. Because of this issue, MIPs prepared using the common bulky polymerization technique are not useful for proteins and other macromolecules [5]. Moreover, the protein molecules can be trapped deeply in the polymer matrix, which is resulting in a deteriorated elution [18,19]. Surface imprinting via nanoscale carrier materials is well suited for proteins as a template, considering the mentioned problems [15]. Moreover, the conditions here can be adapted more to the properties of the proteins. In the present study, core-shell imprinting was selected, which is a special application of the surface imprinting technique. Commonly used support materials for surface imprinting technique are TiO₂, [20] Fe₂O₃, [21] and carbonaceous materials [22]. However, SiO₂ was the most frequently used solid support material reported by numerous studies [5]. However, protein imprinting is still in the early stage, mainly because of the poor stability of the template protein during the polymerization, their limited solubility and stability (i.e., pH, temperature, etc.), as well as structural flexibility in solution [23].

Because biological macromolecules show a poor solubility and tend to change their conformational structure with their loss of biological activity in organic solvents, the imprinting is usually performed in aqueous environments. Due to the fact that many functional monomers are better soluble in organic solvents, the number of suitable monomers is limited [15].

The protein used as a template in our study was the Hen egg white (HEW) lysozyme. HEW lysozyme consists of 129 amino acids, with a molar mass of 14.3 kDa. It is a single peptide chain protein and contains 4 pairs of cysteines on the molecule forming 4 S-S bonds. The lysozyme is elliptical and has a size of 4.5 nm × 3.0 nm × 3.0 nm. The isoelectric point is at pI 11.35. Lysozyme exhibits a globular structure composed of four α -helices and five β -sheets, with four disulfide bridges [24]. The enzyme is active over a wide pH range (6.0 to 9.0). Maximum activity is observed at pH 6.2 [25–28]. The internal structure of lysozyme is almost non-polar, and hydrophobic interactions play an important role in the folded conformation of lysozyme [25,27]. Lysozymes preferentially hydrolyze the β -1,4-glycosidic bond between N-acetyl-D-muramic acid and 2-acetyl-amino-2-deoxy-D-glucose (=N-acetyl-D-glucosamine) in the sugar chains of the peptidoglycan scaffold of the bacterial cell wall. As a result, these enzymes have antibacterial properties. Lysozyme is abundant in a number of biological secretions, such as saliva, tears, sweat, human milk, earwax, and nasal and intestinal mucosa, as well as in blood plasma. Large amounts of lysozyme are found in hen egg white. In food industries, HEW lysozyme is approved within the EU as a food additive (i.e., number E 1105). For example, it is used at concentrations of up to 50 g/hl in winemaking to control acid biodegradation (i.e., bacterial breakdown of malic acid into lactic acid). Furthermore, it is used as a conservation agent for aged cheese and to preserve beer that has not been pasteurized or sterile-filtered [25–27]. For these reasons, it is necessary to be able to isolate and purify lysozyme. A common method for this so far is pH precipitation (salting out) and via chromatography on a cation exchange column. The salting-out process, based on the addition of a neutral salt, compresses the solvation layer and increases protein–protein interactions. When the salt concentration of a solution is enhanced, the charges on the surface of the protein interact with the salt, not with the water, exposing hydrophobic regions on the protein surface and causing the protein to precipitate out of solution [29]. The isoelectric point (pI) also plays an important role in this process. If the pH conforms to the pI, the protein has no netto charge. The negative and positive charges balance each other out, which reduces the repulsive electrostatic forces so that the attractive forces prevail. The attractive forces lead to aggregation and precipitation [29]. Thus, the solubility is the lowest at or close to this point. Lysozyme has a minimum solubility at around pH 10 [29]. This state of precipitation can be partially irreversible, so that the protein denatures. Moreover, the high pH can also lead to denaturation. This point is a disadvantage of this method [29]. Furthermore, the cation exchange chromatography works with the pI of the proteins. It can separate molecules based on their netto surface charge [30]. For this device, it is important that the target molecule, in this case lysozyme,

has a positive surface charge. Thus, a pH of below 9 is required. This method involves several steps: the buffer preparation, the column equilibration, the sample loading, the column washing and the elution of the protein [30,31]. This involves a certain amount of effort. Furthermore, the effectiveness of this method is also highly pH dependent, if the pH is too close to the pI the amount of positive charges decreases. Moreover, to separate several proteins from each other using this method a salt gradient is then used to separate the protein of interest from other bound proteins, so they will be eluted in an order depending on their net surface charge [30,31]. This requires knowledge about their pIs. These points make this method more sophisticated in its usage. MIPs have the potential to represent an alternative, inexpensive method for lysozyme purification.

2. Materials and Methods

2.1. Chemicals

Acrylamide (AAM; $\geq 99\%$; Product No. A3553), Ammonium persulfate (APS; 98%; Product No. 215589), Hexadecyltrimethylammonium bromide (CTAB; $\geq 99\%$; Product No. H6269), Lysozyme from chicken egg white (HEW Lyz; $\geq 90\%$; Product No. L6876), Methacrylic acid (MAA; 99%; Product No. 155721), *N,N'*-Methylenbisacrylamide (MBA; 99%; Product No. 146072), *N,N,N',N'*-Tetramethylethylenediamine (TEMED; 99%; Product No. T22500), Sodium Citrate tribasic dihydrate ($\geq 99\%$; Product No. 71405), Thermolysin from *Geobacillus stearothermophilus* (Therm; Product No. T7902) and Trypsin from bovine pancreas (Tryp; Product No. T8003) were purchased from Sigma Aldrich (Steinheim, Germany). (3-Aminopropyl)-triethoxysilane, (APTES; 98%; Product No. A10668), (3-Aminopropyl)-trimethoxysilane (APTMS; 97%; Product No. A11284) and Hydrochloric acid solution (HCl; 1M; Product No. 35640) were acquired by purchase from Alfa Aesar (Kandel, Germany). Ammonia solution (28–30%; Product No. 1.05423) and Ethanol (99.5%; Product No. 8.5033) were obtained from VWR International. Citric acid trisodium salt dihydrate (99%; Product No. A12274) was purchased from Acros organics (Geel, Belgium). 2-(Dimethylamino)-ethyl methacrylate (DMAEMA; $\geq 99\%$; Product No. 8.40083), Dimethylformamide (DMF; 99.9%; Product No. 1.02375), di-Sodium hydrogen phosphate 2-hydrate ($\geq 99.5\%$; Product No. 1.06580), Glutaraldehyde (50% solution in water; Product No. 8.14393), Potassium Chloride ($\geq 99.5\%$; Product No. 1.04933), Potassium di-hydrogen phosphate ($\geq 99.0\%$; Product No. P0662), Sodium Chloride ($\geq 99.5\%$; Product No. 1.06404) and Tetraethyl orthosilicate ($\geq 99\%$; Product No. 8.00658) were purchased from Merck (Darmstadt, Germany).

2.2. Synthesis of Core-Shell MIP Particles

2.2.1. Synthesis of the Silica Cores

Amino-functionalized silica ($\text{SiO}_2\text{-NH}_2$) cores were synthesized using Stöber synthesis. For this purpose, 30 mL of ammonia solution (28–30%) were mixed with 150 mL ethanol and stirred for 10 min. Simultaneously, a solution of 30 mL ethanol, 4 mL APTES and 2 mL TEOS was prepared and stirred for 5 min. Then, the solutions were combined and stirred for 30 min at 25 °C. This results in silica cores C1. For variation of the core properties, 25 mg Cetyltrimethylammoniumbromide (CTAB) were added to the mixture. However, these modified silica particles denoted as cores C2 were only used in synthesis route I. To finish the reaction, another 50 mL ethanol were added to the solution. The particles were collected by centrifugation (4200 rpm) and washed with ethanol. Finally, the particles were dried overnight in a vacuum oven at 40 °C and 600 mbar.

2.2.2. Synthesis Route I (Organic Shell, OC)

Functionalization of the core surface: To introduce polymerizable double bonds and terminal carboxyl groups onto the core surface of the $\text{SiO}_2\text{-NH}_2$, maleic anhydride was used. For this, the $\text{SiO}_2\text{-NH}_2$ cores (250 mg) were dispersed in 12 mL DMF by ultrasonic. Subsequently, maleic anhydride (315 mg) and pyridine (210 μL) were added, and the mixture was stirred for 3 h at 80 °C. The particles were collected by centrifugation, washed

with ethanol and dried overnight (40 °C and 600 mbar). These particles are denoted as SiO₂-COOH.

Imprinting Step: The crosslinking degree of this route is 50% and the molar ratio of AAM/MAA/DMAEMA is 1/0.12/0.12. The procedure of imprinting was carried out as described below. The SiO₂-COOH particles (120 mg) were dispersed in 35 mL PBS (pH = 7.4) or citrate buffer (pH = 6.2). Then, MBA (80 mg), AAM (57.4 mg), MAA (8 mg), DMAEMA (14.6 mg) and Lyz (32 mg) were added to the suspension. The mixture was shaken for 1 h to obtain the pre-polymerization complex. As a next step, the mixture was purged with argon for 20 min to remove oxygen from solution. By injecting 120 µL APS solution (10 or 20%, (w/v)) and 60 µL of TEMED solution (5%, (v/v)), the polymerization reaction was initiated. The mixture was stirred at 25 °C for 24 h. The obtained particles were collected with centrifugation (2800 rpm) and washed two times with deionized water in order to remove oligomers and unreacted monomers. The obtained particles were washed repeatedly with 0.5 M NaCl solution for template extraction until no Lyz was detected in the supernatant at 280 nm. After re-washing with deionized water to remove the remaining NaCl, the particles were dried overnight (40 °C and 600 mbar). Control polymers (NIPs) were prepared by the same synthesis protocol but in the absence of lysozyme. These core-shell particles have an inorganic (silica) core and an organic shell.

2.2.3. Synthesis Route II (Inorganic Shell, IC)

Functionalization of the core surface: In this route, no linker was required for grafting the polymer layer onto the core surface as the monomers and crosslinkers can be attached directly to the surface. However, to immobilize and orient the lysozyme prior to polymerization, the core particles were functionalized with glutaraldehyde. First, the SiO₂-NH₂ particles (300 mg) were dispersed in 12 mL water using ultrasonic. Then, a surplus of glutaraldehyde (165 µL, 7 µmol/mg particles) was added to the suspension and the mixture was shaken for 30 min at 25 °C. Afterwards, the particles were washed with deionized water and subsequently dried overnight (40 °C and 600 mbar).

Imprinting step: For the imprinting, the functionalized particles (250 mg) were suspended in 20 mL PBS (pH = 7.4) or citrate buffer (pH = 6.2). To the particles, 20 mL of lysozyme solution (2 mg/mL) were added. The particles were incubated with the lysozyme solution by shaking for 1 h. After removing the lysozyme solution, another 20 mL PBS or citrate buffer were added to the particles. Moreover, 4 µL APTES, 4 µL APTMS and 25 µL TEOS were added and the mixture was shaken for 24 h. Control polymers were prepared in the same way, but without the incubation step. These core-shell particles have an inorganic (silica) core and an inorganic (silica) shell.

Table 1 provides an overview to the different synthesis variations and their abbreviations.

Table 1. Abbreviations of the syntheses.

Abbreviation	Synthesis Route	Core Type	APS Solution (w/v)	pH	Extraction
OC1 _{10%}	I	1	10%	7.4	0.5 M NaCl
OC1 _{20%}	I	1	20%	7.4	0.5 M NaCl
OC1 _{Citrate}	I	1	20%	6.2	0.5 M NaCl
OC2 _{PBS}	I	2	20%	7.4	0.5 M NaCl
OC2 _{Citrate}	I	2	20%	6.2	0.5 M NaCl
IC _{PBS}	II	1	-	7.4	1 M HCl
IC _{Citrate}	II	1	-	6.2	1 M HCl

In total, 5 variants of synthesis route I (OC) were successfully synthesized. Of these, 3 had silica particles C1 as the core (OC1), while 2 variants owned silica particles C2 as the core (OC2). Furthermore, 2 variants of synthesis route II were prepared (IC), both using silica particles C1 as core.

2.3. Protein Rebinding Experiments

For the investigation of the obtained rebinding properties (binding kinetics, binding capacity and selectivity) of the core-shell particles, incubation rebinding experiments were examined. For this purpose, 10 mg of dried particles were suspended in 750 μ L of 0.5–1.0 mg/mL protein solutions prepared using PBS (pH = 7.4) or citrate buffer (pH = 6.2) as a solvent. The standard incubation time was 30 min. Competitive binding studies testing selectivity using trypsin and thermolysin were performed in the same way using a protein solution with the concentration 1.0 mg/mL. All studies were performed at room temperature. The amount of adsorbed protein by the nanoparticles after the rebinding experiments was calculated using the following formula:

$$q = \frac{(c_i - c_f) \cdot V}{m}$$

where q (mg/g) is the mass of protein adsorbed by unit mass of dry particles, c_i (mg/mL) and c_f (mg/mL) are the protein concentrations of the initial and the final solutions. V (mL) is the total volume of the mixture, while m is the mass of the applied particles.

2.4. Particle Characterization

Scanning electron microscopy (SEM) images were taken on a Quanta 3D FEG (FEI Company USA, Hillsboro, OR, USA) operated at 3.00 kV. The Brunauer–Emmett–Teller (BET) measurements were performed on a Quatrasorb SI/Quararorb evo (Quantachrome/3P-Instruments, Odelzhausen, Germany). The Dynamic Light Scattering (DLS) experiments were carried out on a Zetasizer Nano ZS (Malvern Instruments, Malvern, UK). The laser has a wavelength of 633 nm and the measurements were taken at an angle of 173°. All UV-Vis measurements were taken on a Specord S600 (Analytik Jena, Jena, Germany) at 280 nm.

3. Results

3.1. DLS Studies

Table 2 summarizes the results of the DLS experiments.

Table 2. DLS Results.

Abbreviation	Z-Average d [nm]	PdI
C1	330.60	0.03
C2	416.50	0.01
MIP(OC1 _{10%})	970.60	0.14
NIP(OC1 _{10%})	609.37	0.04
MIP(OC1 _{20%})	1203.33	0.29
NIP(OC1 _{20%})	824.03	0.22
MIP(OC1 _{Citrate})	539.33	0.11
NIP(OC1 _{Citrate})	401.87	0.65
MIP(OC2 _{PBS})	873.37	0.34
NIP(OC2 _{PBS})	825.97	0.42
MIP(OC2 _{Citrate})	481.20	0.13
NIP(OC2 _{Citrate})	432.50	0.06
MIP(IC _{PBS})	1005.00	0.67
NIP(IC _{PBS})	497.37	0.14
MIP(IC _{Citrate})	707.30	0.87
NIP(IC _{Citrate})	341.40	0.28

Table 2 shows that cores C1 have a smaller diameter compared to cores C2, i.e., the addition of CTAB leads to an increase in diameter. Both core particle types have a very small PdI and are nearly monodisperse. The DLS measurements confirm that a polymer layer has formed around the core particles as the diameter has increased in all cases. Furthermore,

the particle diameters of the MIPs are always larger than those of the corresponding NIPs; thus, the polymer layer formed is thicker. It can also be seen that doubling the starter concentration leads to the formation of a thicker polymer layer (see OC1_{10%} and OC1_{20%}). Comparing the OC1_{20%} and OC1_{Citrate} synthesis variants, it can be stated that the diameters are significantly smaller for OC1_{Citrate} as for OC1_{20%}. Larger diameters were also obtained for the OC2 and IC variants in PBS rather than in citrate buffer. Thus, pH has an influence on the thickness of the polymer layer. Particles C1 also result in MIP/NIP pairs whose diameters sometimes diverge by a factor of 2. The MIP/NIP pairs of particles C2, on the other hand, have similar diameters.

3.2. BET Studies

Table 3 shows the results of the BET measurements.

Table 3. BET results.

Abbreviation	Surface Area (Adsorption) (m ² /g)	Pore Diameter (Adsorption) (nm)	Pore Volume (Adsorption) (cc/g)
C1	12.16	12.88	0.06
C2	11.48	3.87	0.04
MIP(OC1 _{10%})	13.87	4.66	0.05
NIP(OC1 _{10%})	50.07	3.00	0.10
MIP(OC1 _{20%})	34.48	3.54	0.08
NIP(OC1 _{20%})	21.86	3.74	0.07
MIP(OC1 _{Citrate})	18.14	3.01	0.04
NIP(OC1 _{Citrate})	12.95	3.49	0.04
MIP(OC2 _{PBS})	22.76	3.32	0.07
NIP(OC2 _{PBS})	24.84	4.17	0.07
MIP(OC2 _{Citrate})	41.81	5.77	0.09
NIP(OC2 _{Citrate})	92.85	3.66	0.15
MIP(IC _{PBS})	28.73	3.51	0.06
NIP(IC _{PBS})	11.96	3.66	0.04
MIP(IC _{Citrate})	17.57	8.04	0.11
NIP(IC _{Citrate})	17.42	4.11	0.09

From Table 3 it is evident that the surface properties of the bare silica particles are influenced by their composition. The deviating pore diameters are particularly noticeable here. However, depending on the pore diameter, not the entire surface is available for adsorption of lysozyme. As mentioned, the dimensions of lysozyme are 4.5 nm × 3.0 nm × 3.0 nm. Taking this fact into account, lysozyme can diffuse more easily into the pores of particles C1 than into the pores of cores C2. For all MIPs and NIPs which have silica particles C1 as their core, it can be established that the pore diameters were significantly decreased (factor 3–4). On the basis of this fact, it can be assumed that polymer has built up in the pores resulting in a reduced pore diameter. For both cores C1 and C2, the surface areas increased after the imprinting step (with exception of NIP(IC_{PBS}), revealing a slight decrease). Since there is a change in surface properties for all variations, it can be assumed that a polymer layer has formed at the particles.

3.3. SEM Studies

Figure 1 provides a comparison between the core particles C1 and C2.

Particles C1 are spherical, with a narrow size distribution. Their average size is 330.60 nm (see Table 2). The particles are non-agglomerated and have no visible pores. Based on the BET measurements (see Table 3), it is evident that these particles have small pores with an average diameter of 12.88 nm. Particles C2 appear slightly more inhomogeneous in shape, but otherwise there are no visible differences to particles C1. Their average size is 416.50 nm (see Table 2) and they have also a narrow size distribution. These particles also have no evident pores with the determined pore diameter averaging 3.87 nm (compare Table 3).

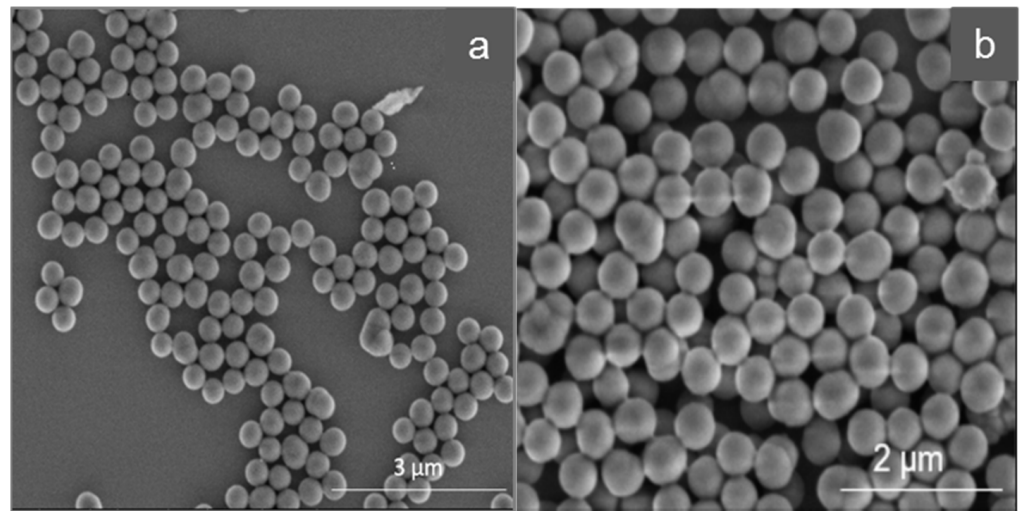


Figure 1. Comparison of the silica core particles (SEM images), (a): cores C1, (b): cores C2.

Figure 2 shows exemplary the SEM images of MIP and NIP OC1_{Citrate}.

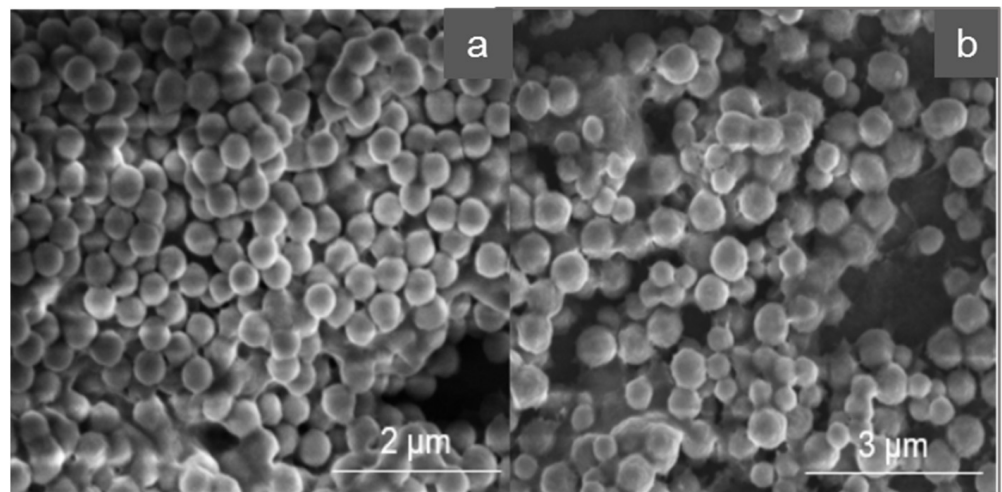


Figure 2. SEM images of MIP (a) and NIP (b); variant OC1_{Citrate}.

Compared to the initial particles C1 (see Figure 1), the surface of MIP and NIP appears significantly modified. The surface of the core-shell polymers is corrugated and it is evident that a polymer coating has been formed both at the surface and between particles. In addition, MIP and NIP have a larger diameter than the initial particles C1. The modification of the surface was verified via DLS and BET measurements (compare Tables 2 and 3). The MIPs are slightly more agglomerated than the NIPs.

3.4. Synthesis Route I (OC)

A schematic representation of synthesis route I is depicted in Figure 3.

3.4.1. Polymers OC1_{10%}

To gain an insight into binding kinetics, rebinding studies were carried out at incubation times of 30 min, 60 min and 240 min. Thereby, 1.0 mg/mL was chosen as initial the lysozyme concentration. The study was performed in PBS. Table 4 shows the results.

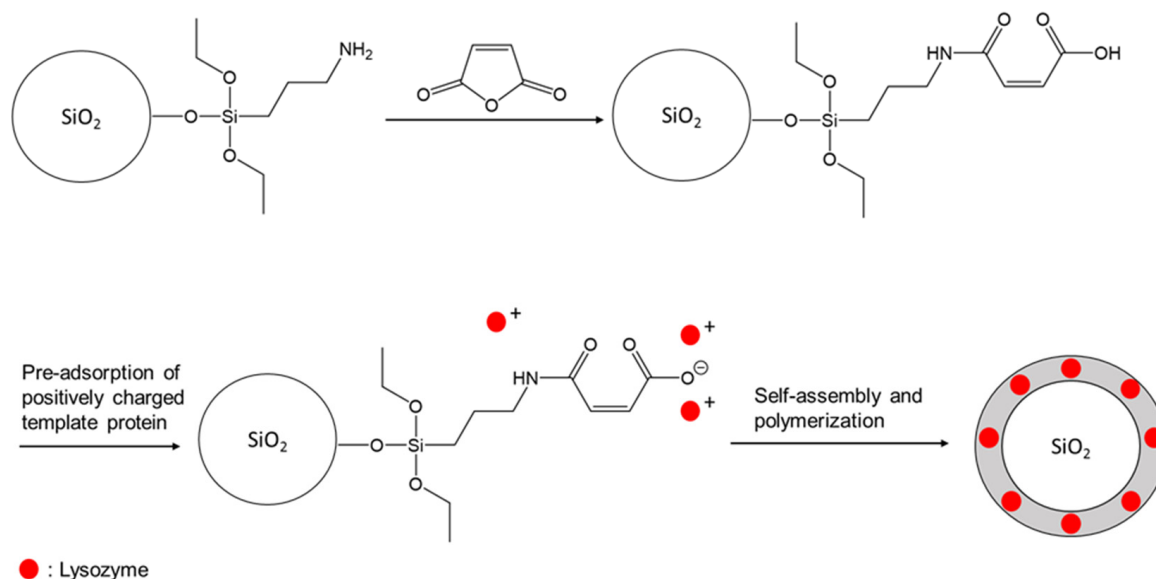


Figure 3. Synthesis route I (organic polymeric shell).

Table 4. Results of time dependent rebinding study of polymers OC1_{10%} in PBS.

Incubation Time (min)	Q _{MIP} (mg/g)	Q _{NIP} (mg/g)	IF (a.u.)
30	43.59	33.83	1.29
60	23.38	20.35	1.14
240	2.9	19.53	0.15

Table 4 shows that only the incubation times of 30 min and 60 min result in an imprinting factor higher than 1. It is also noticeable that Q_{MIP} and imprinting factor continue to decrease with increasing incubation time and the best values are obtained after only 30 min. Thus, if the incubation period is too long, the number of non-specific bindings increases and outweighs the specific ones, resulting in a lower imprinting factor. Therefore, 30 min was chosen as the standard incubation time.

To analyze the influence of the lysozyme concentration on the binding properties, a concentration-dependent study was performed in PBS.

Table 5 summarizes the results of this study.

Table 5. Results of concentration dependent rebinding study of polymers OC1_{10%} in PBS.

Lysozyme Concentration (mg/mL)	Q _{MIP} (mg/g)	Q _{NIP} (mg/g)	IF (a.u.)
0.5	2.36	1.45	1.63
0.75	3.14	1.14	2.74
1.0	43.59	33.83	1.29

Q_{MIP} rise with increasing lysozyme concentration with a rapid gain between 0.75 mg/mL and 1.0 mg/mL. All imprinting factors are larger than 1, the highest imprinting factor is obtained at the initial concentration of 0.75 mg/mL. Nonspecific binding is assumed to be the reason for the decrease to higher concentrations.

3.4.2. Polymers OC1_{20%}

As the next step, the concentration of the initiator (APS solution) was doubled, resulting in variant OC1_{20%}. With these polymers, concentration-dependent rebinding studies were performed in PBS and citrate buffer to check the influence of both lysozyme concentration and pH during the rebinding process.

Table 6 summarizes the results for the concentration-dependent rebinding studies.

Table 6. Results of concentration dependent rebinding study of polymers OC1_{20%}.

Lysozyme Concentration (mg/mL)	Q _{MIP} (mg/g)	Q _{NIP} (mg/g)	IF (a.u.)	pH
0.5	14.81	8.16	1.82	7.4
0.75	21.77	17.42	1.25	7.4
1.0	35.73	31.95	1.12	7.4
0.5	18.80	12.13	1.55	6.2
0.75	25.05	15.99	1.57	6.2
1.0	46.28	37.07	1.25	6.2

Comparing the results in PBS with those from variant OC1_{10%}, Q_{MIP} increased significantly for the lysozyme concentrations 0.5 mg/mL and 0.75 mg/mL, while it decreased slightly for 1.0 mg/mL (compare with Table 5). For 0.5 mg/mL, the imprinting factor increased in this synthesis variant, while the opposite can be observed for the higher concentrations.

Both for PBS and citrate buffer, Q_{MIP} increases with the increasing lysozyme concentration, while the imprinting factors follow the opposite trend. Therefore, it is evident that the specific binding sites are already largely occupied at lower concentrations, and non-specific bonds are formed at higher concentrations. However, their influence is in general less pronounced in citrate buffer than in PBS. It may be observed that the specific binding capacities Q_{MIP} are higher in citrate buffer than in PBS; these observations could be due to the fact that this pH corresponds to the point of maximum activity of the lysozyme.

Thus, in direct comparison, pH = 6.2 proves to be more advantageous, at least for this synthesis variant.

A graphical comparison of the imprinting factors in both buffers is shown in Figure 4.

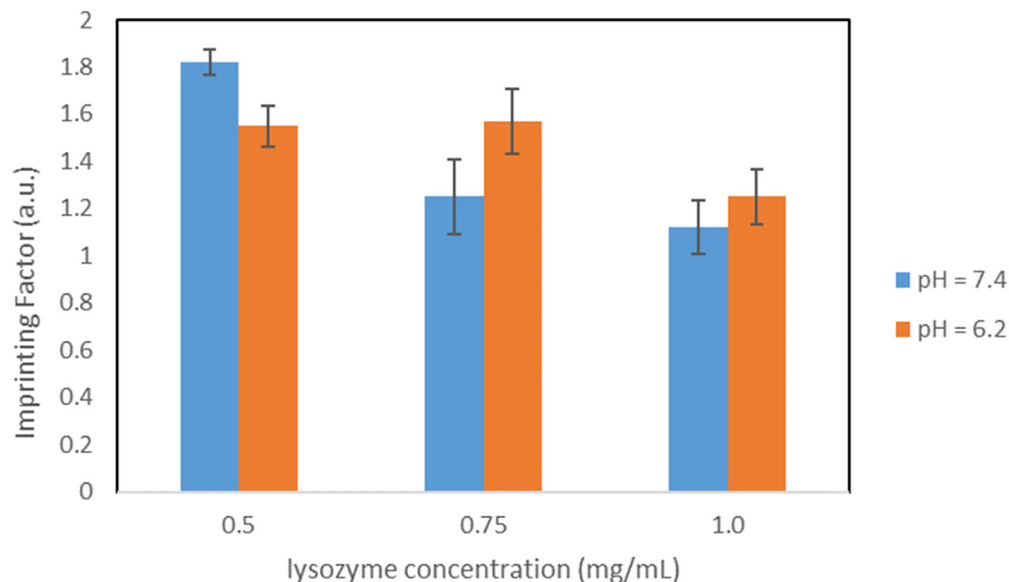


Figure 4. Comparison of the IFs, particles OC1_{20%}.

In order to verify the selectivity of the polymers, a comparative study was carried out in citrate buffer. The results are shown further down.

3.4.3. Polymers OC1_{Citrate}

To determine whether the pH during the synthesis has an influence on the binding quality of the polymers, citrate buffer was investigated as solvent instead of PBS resulting in synthesis variation OC1_{Citrate}. All other synthesis parameters correspond to synthesis

variant OC1_{20%}. The results of the concentration dependent study in citrate buffer are shown in Table 7.

Table 7. Results of concentration dependent rebinding study of polymers OC1_{Citrate} in citrate buffer.

Lysozyme Concentration (mg/mL)	Q _{MIP} (mg/g)	Q _{NIP} (mg/g)	IF (a.u.)
0.5	24.36	21.73	1.12
0.75	42.93	22.09	1.94
1.0	55.32	23.35	2.37

The results conclude that Q_{MIP} correlate with the initial concentration, i.e., the higher the initial lysozyme concentration, the higher the Q_{MIP}. The same trend can be observed for the imprinting factors. Since neither Q_{MIP} nor imprinting factors passed through a maximum, the particles are still specific even at higher lysozyme concentrations. Furthermore, it can be deduced that many specific binding sites were formed that were not yet completely occupied even at 1.0 mg/mL. Compared with the same study of the analog synthesis variant OC1_{20%} (see Table 6), this variant provides better binding properties. Thus, higher Q_{MIP} was achieved at all concentrations. A graphical comparison of the imprinting factors of polymers OC1_{20%} and OC1_{Citrate} in citrate buffer can be seen in Figure 5.

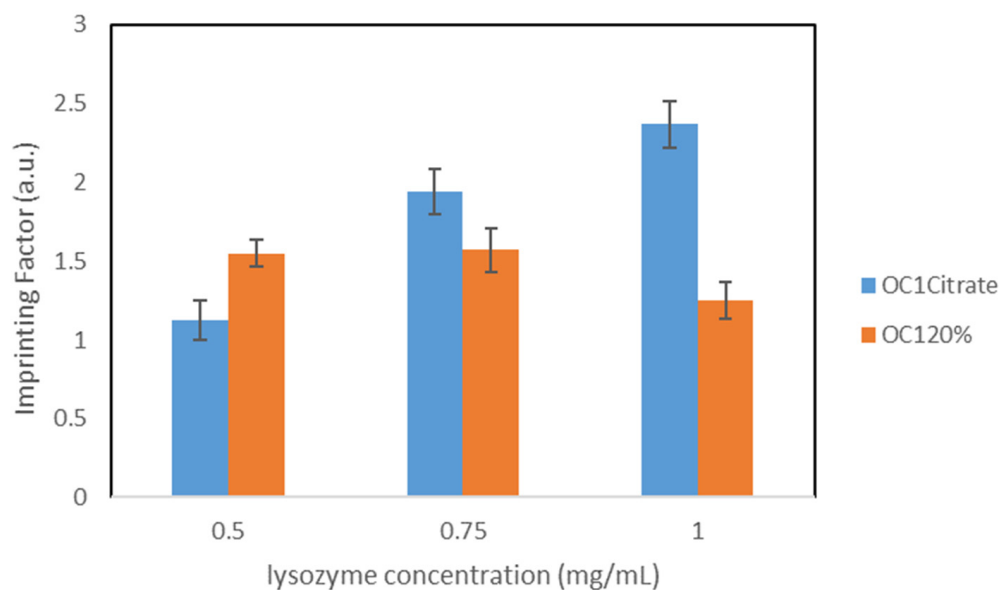


Figure 5. IFs for Particles OC1_{20%} and OC1_{Citrate}, pH = 6.2.

With the exception of 0.5 mg/mL, the imprinting factors rise using polymers OC1_{Citrate}. This optimization can be attributed to the fact that the pH during synthesis corresponds to the optimum of lysozyme activity. This synthesis variant provides a promising approach with respect to the objective of this work. Moreover, good binding characteristics are observed here even at high lysozyme concentrations.

Likewise, a competitive study was performed in citrate buffer, and the results are presented in a latter chapter.

3.4.4. Polymers OC2_{PBS} and OC2_{Citrate}

To gain an insight into the influence of the silica core on the binding properties, the silica core was modified by adding 25 mg CTAB during the Stöber synthesis. This results in the OC2 variants. All other synthesis parameters were retained. Both buffers were tested during the synthesis.

Polymers OC2_{PBS}

The results for the concentration dependent studies both in PBS and citrate buffer are shown in Table 8.

Table 8. Results of concentration dependent rebinding study of polymers OC2_{PBS}.

Lysozyme Concentration (mg/mL)	Q _{MIP} (mg/g)	Q _{NIP} (mg/g)	IF (a.u.)	pH
0.5	31.17	25.13	1.24	7.4
0.75	41.87	22.62	1.85	7.4
1.0	38.05	22.49	1.69	7.4
0.5	28.61	20.24	1.41	6.2
0.75	32.92	28.05	1.17	6.2
1.0	52.46	21.40	2.45	6.2

In PBS, both IF and Q_{MIP} follow the same trend: a maximum can be observed at the concentration 0.75 mg/mL. If this study is now compared with the analogous study with the polymers OC1_{20%} (identical synthesis, different silica core), better results are obtained (compare Table 6). Q_{MIP} of the OC2_{PBS} polymers are higher in all concentrations. Similarly, this variant has better imprinting factors at high lysozyme concentrations. At low concentrations, on the other hand, the OC1_{20%} variant is preferable, since the imprinting factor here is significantly higher and thus the proportion of non-specific binding is smaller. In citrate buffer, on the other hand, the imprinting factor is highest for the initial lysozyme concentration of 1.0 mg/mL. The imprinting factors do not behave proportionally to the initial concentrations, a minimum can be seen at 0.75 mL/mL. Q_{MIP} grows with increasing concentration, and the highest value was received for 1.0 mg/mL.

The highest Q_{MIP} and imprinting factor for the OC2_{PBS} variant were both obtained in citrate buffer for a lysozyme concentration of 1.0 mg/mL. Figure 6 compares the concentration dependent IFs during both pH values.

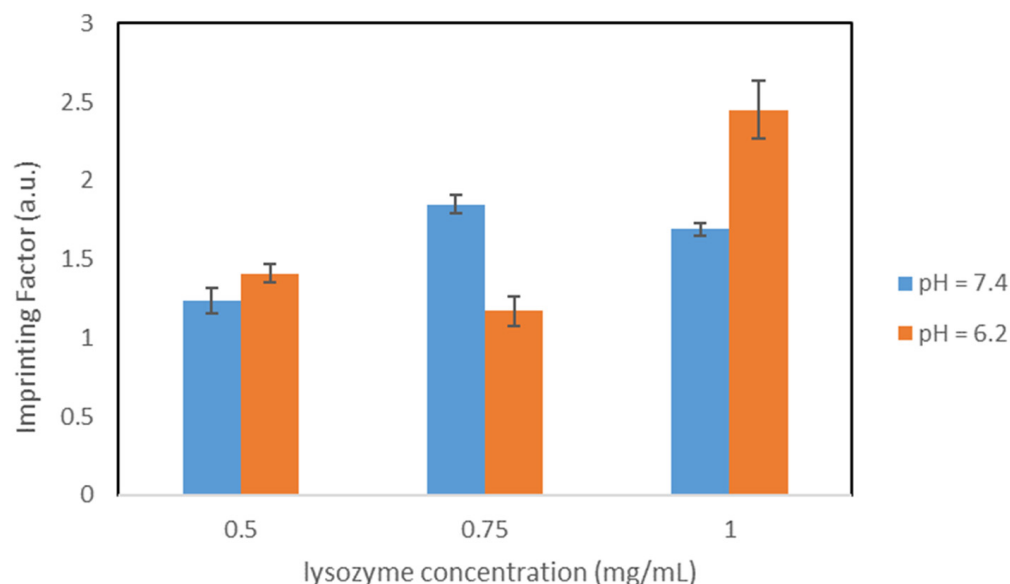


Figure 6. Comparison of the IFs, particles OC2_{PBS}.

Comparing both buffers for variant OC2_{PBS}, it can be stated that citrate buffer is better qualified for higher lysozyme concentrations. PBS tends to be better suited for lower lysozyme concentrations, since higher Q_{MIP} were obtained here.

Comparing this study in citrate buffer with the analogous study with the particles OC1_{20%} (see Table 6) can be established that Q_{MIP} increases for all concentrations. The opposite trend

can be observed for the IFs (for the concentrations 0.5 mg/mL and 0.75 mg/mL). For the concentration 1.0 mg/mL, on the other hand, the imprinting factor is almost doubled.

The results for the competitive study in citrate buffer can be found subsequent.

Polymers OC2_{Citrate}

The results for the concentration dependent studies in PBS and citrate buffer are shown in Table 9.

Table 9. Results of concentration dependent rebinding study of polymers OC2_{Citrate}.

Lysozyme Concentration (mg/mL)	Q _{MIP} (mg/g)	Q _{NIP} (mg/g)	IF (a.u.)	pH
0.5	26.80	23.30	1.15	7.4
0.75	58.82	24.80	2.37	7.4
1.0	57.35	26.02	2.20	7.4
0.5	28.61	20.24	1.44	6.2
0.75	26.85	13.47	1.99	6.2
1.0	46.17	37.06	1.25	6.2

For these polymers in PBS, both the highest imprinting factor and Q_{MIP} were obtained for the initial lysozyme concentration 0.75 mg/mL. However, the decrease in both quantities to the concentration 1.0 mg/mL is relatively minor. In contrast, significantly poorer binding properties were obtained for 0.5 mg/mL. These two aspects make this variant in PBS more applicable for higher lysozyme concentrations. Moreover, in citrate buffer, the highest imprinting factor was obtained at 0.75 mg/mL, while the highest Q_{MIP} is obtained for 1.0 mg/mL. The imprinting factors decrease sharply between 0.75 mg/mL and 1.0 mg/mL indicating an increase in non-specific binding to high concentrations.

Figure 7 compares the imprinting factors of particles OC2_{Citrate} in both buffers.

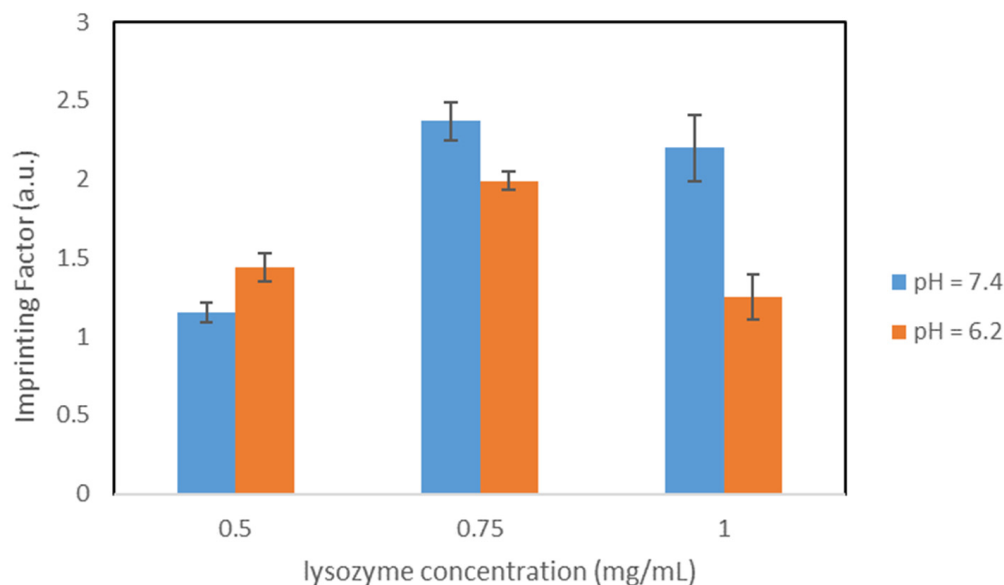


Figure 7. Comparison of the IFs, particles OC2_{Citrate}.

However, higher imprinting factors were obtained for 0.75 mg/mL and 1.0 mg/mL in PBS rather than in citrate buffer. For 0.5 mg/mL, on the other hand, an increase in both Q_{MIP} and imprinting factor is observed in citrate buffer.

When the results in citrate buffer are compared with the analogous study with particles OC1_{Citrate} (see Table 7), it is shown that the imprinting factors for the two smaller concentrations have increased, while the imprinting factor for 1.0 mg/mL has nearly halved. For the two higher concentrations, Q_{MIP} decreased compared to the OC1_{Citrate} variant.

Table 10 compiles the results of the completed studies.

Table 10. Results of the comparative studies of polymers OC1_{20%}, OC1_{Citrate}, OC2_{PBS} and OC2_{Citrate} in citrate buffer.

Protein	Q _{MIP} (mg/g)	Q _{NIP} (mg/g)	Polymers	pH
Lysozyme	46.28	37.07	OC1 _{20%}	6.2
Trypsin	38.65	32.99	OC1 _{20%}	6.2
Thermolysin	31.92	20.79	OC1 _{20%}	6.2
Lysozyme	55.32	23.35	OC1 _{Citrate}	6.2
Trypsin	59.19	48.06	OC1 _{Citrate}	6.2
Thermolysin	37.94	30.26	OC1 _{Citrate}	6.2
Lysozyme	52.46	21.40	OC2 _{PBS}	6.2
Trypsin	52.95	37.89	OC2 _{PBS}	6.2
Thermolysin	41.10	23.53	OC2 _{PBS}	6.2
Lysozyme	46.17	37.06	OC2 _{Citrate}	6.2
Trypsin	25.87	11.08	OC2 _{Citrate}	6.2
Thermolysin	37.07	35.08	OC2 _{Citrate}	6.2

It is noticeable that the target protein lysozyme binds better to the OC1_{20%} MIP than the reference proteins. Thus, it can be concluded that the polymer particles show a degree of selectivity in citrate buffer.

For the OC1_{Citrate} variant, the MIP binds the lysozyme better than thermolysin, and so there is a selectivity towards thermolysin. However, trypsin is bound slightly better by particles OC1_{Citrate} than by lysozyme. It is noteworthy that the ratio of the binding capacities between MIP and NIP is more pronounced for lysozyme than for both reference proteins. For the OC2_{PBS} version it applies that trypsin is best bound by MIP, but the difference with lysozyme is negligible. Thermolysin is less bound by the MIPs. For OC_{Citrate}, Q_{MIP} is significantly larger for lysozyme than for trypsin and thermolysin. The particles are thus selective.

3.5. Synthesis Route II (IC)

A schematic representation of synthesis route II is depicted in Figure 8.

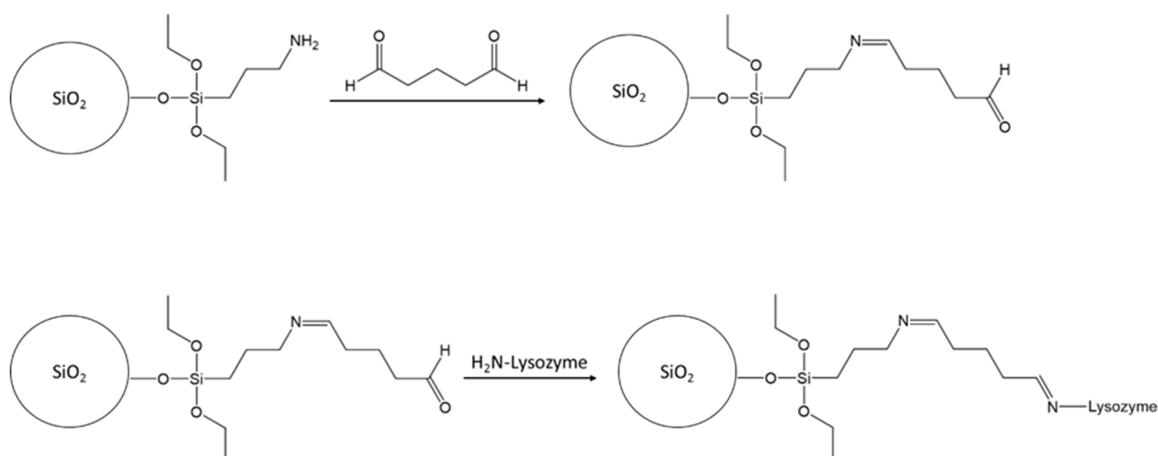


Figure 8. Synthesis route II (inorganic silica shell).

This synthesis was also performed in PBS and citrate buffer.

3.5.1. Polymers IC_{PBS}

The results for the concentration dependent study in PBS are shown in Table 11.

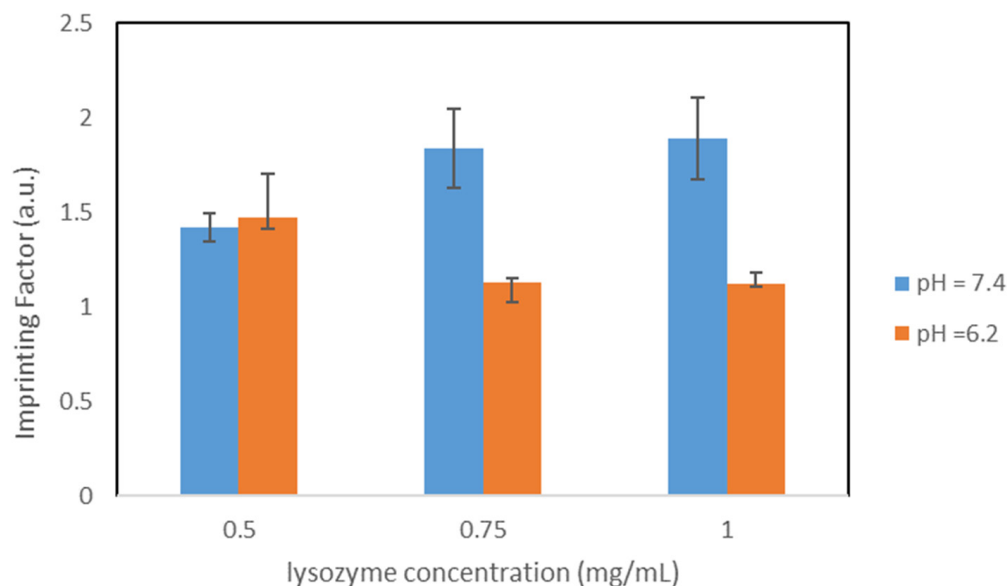
Table 11. Results of concentration dependent rebinding study of polymers IC_{PBS}.

Lysozyme Concentration (mg/mL)	Q _{MIP} (mg/g)	Q _{NIP} (mg/g)	IF (a.u.)	pH
0.5	25.65	18.08	1.42	7.4
0.75	32.47	17.68	1.84	7.4
1.0	36.77	19.49	1.89	7.4
0.5	31.57	21.30	1.48	6.2
0.75	33.73	29.87	1.13	6.2
1.0	41.07	36.70	1.12	6.2

In PBS, both Q_{MIP} and imprinting factors increase with increasing lysozyme concentration, no maximum was reached for both parameters in the investigated concentration range. Thus, the non-specific binding does not have a considerable influence here.

As in PBS, Q_{MIP} rises in citrate buffer with increasing lysozyme concentration, but reaches higher values. However, since the imprinting factors decrease with increasing lysozyme concentration, this gain can be attributed to non-specific binding.

Figure 9 represents the IF for the different concentrations for both pH values.

**Figure 9.** Comparison of the IFs, particles IC_{PBS}.

The highest imprinting factor for these particles is obtained in PBS at lysozyme concentration 1.0 mg/mL. For smaller lysozyme concentrations, it is thus advantageous to use the polymers in citrate buffer, since the imprinting factor and Q_{MIP} are higher here. For higher concentrations (0.75 mg/mL and 1.0 mg/mL), PBS is better suited.

3.5.2. Polymers IC_{Citrate}

Table 12 shows the results of the concentration-dependent study in PBS.

In PBS, Q_{MIP} grows with increasing lysozyme concentration. However, the highest imprinting factor is obtained for the lysozyme concentration 0.75 mg/mL, so the proportion of non-specific binding increases at higher concentrations. Comparing this study with the analog synthesis (particles IC_{PBS} in PBS, see Table 13) it can be noted that Q_{MIP} has increased for all concentrations. The opposite can be observed for the IF. This leads to the conclusion that the growth of Q_{MIP} is due to a high proportion of non-specific binding.

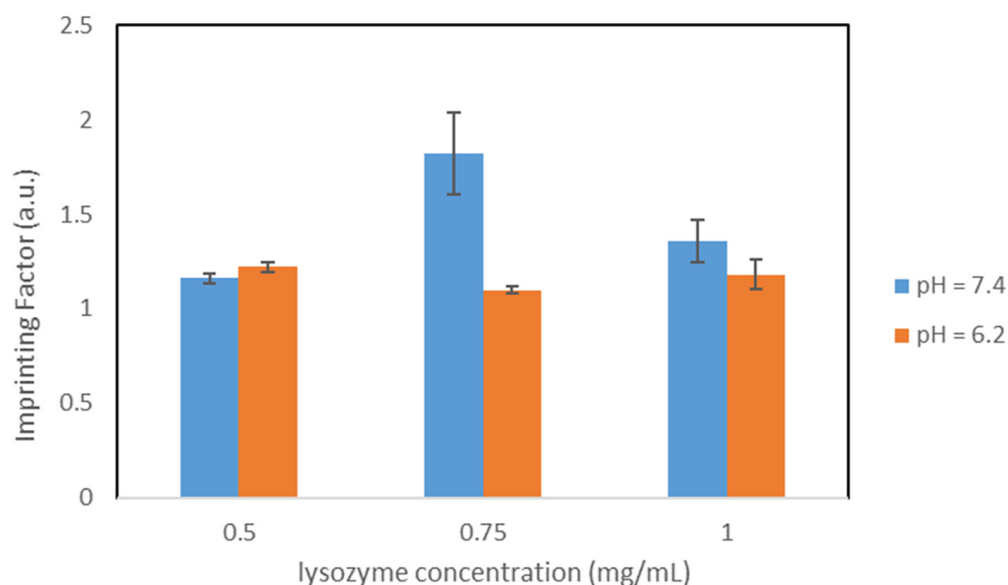
Table 12. Results of concentration dependent rebinding study of polymers IC_{Citrate} in PBS.

Lysozyme Concentration (mg/mL)	Q _{MIP} (mg/g)	Q _{NIP} (mg/g)	IF (a.u.)	pH
0.5	27.53	23.64	1.16	7.4
0.75	41.12	22.59	1.82	7.4
1.0	47.40	34.91	1.36	7.4
0.5	23.40	19.16	1.22	6.2
0.75	33.72	30.55	1.10	6.2
1.0	46.64	39.50	1.18	6.2

Table 13. Results of the comparative study of polymers IC_{Citrate} in PBS.

Protein	Q _{MIP} (mg/g)	Q _{NIP} (mg/g)	pH
Lysozyme	47.40	34.91	7.4
Trypsin	45.51	44.03	7.4
Thermolysin	39.14	32.16	7.4

Moreover, in citrate buffer, Q_{MIP} increases with growing lysozyme concentration; however, the highest imprinting factor is obtained for 0.5 mg/mL. A plot comparison of the obtained imprinting factors is shown in Figure 10.

**Figure 10.** Comparison of the IFs, particles IC_{Citrate}.

The highest imprinting factor for these polymers is obtained in PBS at 0.75 mg/mL. At higher lysozyme concentrations higher Q_{MIP} and imprinting factors were received in PBS. Thus, PBS is more suitable for higher lysozyme concentrations.

Q_{MIP} of lysozyme is higher than for the reference proteins. However, the difference to trypsin is minimal. Thus, a degree of selectivity can be assumed. What is noticeable here is that the ratio of Q_{MIP} and Q_{NIP} for lysozyme is better than it is for the reference proteins.

In conclusion, Q_{MIP} has increased with increasing lysozyme concentration for both variants in both buffers.

Both IC_{PBS} and IC_{Citrate} exhibit higher IF in PBS than in citrate buffer at higher lysozyme concentrations (0.75 mg/mL and 1.0 mg/mL).

4. Conclusions

The present study provides an insight into the development of molecularly imprinted polymers for HEW lysozyme. Using the core-shell approach, specific synthetic receptors

for the model protein were successfully generated. By adjusting the conditions, satisfactory imprinting efficiency with respect to both imprinting factors and binding capacities was achieved. Thus, this method represents a promising alternative to current methods for the isolation of lysozyme. Furthermore, the imprinted particles showed fast rebinding kinetics. As for selectivity, the highest imprinting factor of the core-shell polymers I was 2.74, and for core-shell polymers II 1.89. Thus, a higher sensitivity to lysozyme was achieved using route I. Furthermore, route I achieved better selectivity towards trypsin and thermolysin than route II. The highest Q_{MIP} obtained for route I was 55.32 mg/g (C1 core) and 58.82 mg/g (C2 core), respectively. The highest Q_{MIP} received for route II was 47.40 mg/g.

Thus, the purpose of this study (i.e., high Q_{MIP} and high IF for lysozyme) was maximized via route I vs. route II. Nevertheless, the obtained results for route II were also satisfactory providing slightly less, but still high binding capacities and distinct selectivity. Last, but not least, the latter synthesis route is experimentally easier and less time-consuming, which may be decisive parameters for a scaled-up synthesis required by industrial application scenarios. We compared the results with the work of Zhang and others, where an imprinting factor of 2.53 was achieved. As for route II, this polymer is a silica-based polymer.

Author Contributions: Conceptualization, B.M., M.D. and A.K.; methodology, A.K. and M.D.; formal analysis, A.K.; investigation, A.K.; resources, B.M.; writing—original draft preparation, A.K.; writing—review and editing, B.M. and M.D.; visualization, A.K.; supervision, B.M. and M.D.; project administration, B.M.; funding acquisition, B.M.; All authors have read and agreed to the published version of the manuscript.

Funding: This research was in part funded by the Ministerium für Wissenschaft, Forschung und Kunst (MWK) Baden-Württemberg, Germany, under the Program “Special Measures against the SARS-CoV-2 Pandemic”.

Institutional Review Board Statement: Not applicable.

Informed Consent Statement: Not applicable.

Data Availability Statement: Data will be made available upon request.

Acknowledgments: This work was in part supported by the Ministerium für Wissenschaft, Forschung und Kunst (MWK) Baden-Württemberg, Germany, under the Program “Special Measures against the SARS-CoV-2 Pandemic”.

Conflicts of Interest: The authors declare no conflict of interest.

References

1. Haupt, K.; Mosbach, K. Molecularly Imprinted Polymers and Their Use in Biomimetic Sensors. *Chem. Rev.* **2000**, *100*, 2495–2504. [[CrossRef](#)] [[PubMed](#)]
2. Marty, J.D.; Mauzac, M. Molecular Imprinting: State of the Art and Perspectives. In *Microlithography Molecular Imprinting*; Springer: Berlin/Heidelberg, Germany, 2005; Volume 172, pp. 1–35.
3. Bergmann, N.M.; Peppas, N.A. Molecularly imprinted polymers with specific recognition for macromolecules and proteins. *Prog. Polym. Sci.* **2008**, *33*, 271–288. [[CrossRef](#)]
4. Bossi, A.; Bonini, F.; Turner, A.P.F.; Piletsky, S.A. Molecularly imprinted polymers for the recognition of proteins: The state of the art. *Biosens. Bioelectron.* **2007**, *22*, 1131–1137. [[CrossRef](#)]
5. Zhang, C.; Wang, Y.; Zhou, Y.; Guo, J.; Liu, Y. Silica-based surface molecular imprinting for recognition and separation of lysozymes. *Anal. Methods* **2014**, *6*, 8584–8591. [[CrossRef](#)]
6. Wulff, G. Enzyme-like Catalysis by Molecularly Imprinted Polymers. *Chem. Rev.* **2002**, *102*, 1–28. [[CrossRef](#)] [[PubMed](#)]
7. Hilt, J.Z.; Byrne, M.E. Configurational biomimesis in drug delivery: Molecular imprinting of biologically significant molecules. *Adv. Drug Deliv. Rev.* **2004**, *56*, 1599–1620. [[CrossRef](#)]
8. Weiss, R.; Molinelli, A.; Jakusch, M.; Mizaiikoff, B. Molecular imprinting and solid phase extraction of flavonoid compounds. *Bioseparation* **2001**, *10*, 379–387. [[CrossRef](#)]
9. Dinc, M.; Esen, C.; Mizaiikoff, B. Recent advances on core-shell magnetic molecularly imprinted polymers for biomacromolecules. *TrAC Trends Anal. Chem.* **2019**, *114*, 202–217. [[CrossRef](#)]
10. Ge, Y.; Turner, A.P.F. Molecularly Imprinted Sorbent Assays: Recent Developments and Applications. *Chem. Eur. J.* **2009**, *15*, 8100–8107. [[CrossRef](#)] [[PubMed](#)]

11. Jiang, T.; Zhao, L.; Chu, B.; Feng, Q.; Yan, W.; Lin, J.M. Molecularly imprinted solid-phase extraction for the selective determination of 17 β -estradiol in fishery samples with high performance liquid chromatography. *Talanta* **2009**, *78*, 442–447. [CrossRef]
12. Hu, Y.; Li, Y.; Liu, R.; Tan, W.; Li, G. Magnetic molecularly imprinted polymer beads prepared by microwave heating for selective enrichment of β -agonists in pork and pig liver samples. *Talanta* **2011**, *84*, 462–470. [CrossRef]
13. Resmini, M. Molecularly imprinted polymers as biomimetic catalysts. *Anal. Bioanal. Chem.* **2012**, *402*, 3021–3026. [CrossRef]
14. Shen, X.; Zhu, L.; Liu, G.; Tang, H.; Liu, S.; Li, W. Photocatalytic removal of pentachlorophenol by means of an enzyme-like molecular imprinted photocatalyst and inhibition of the generation of highly toxic intermediates. *New J. Chem.* **2009**, *33*, 2278. [CrossRef]
15. Chen, H.; Yuan, D.; Li, Y.; Dong, M.; Chai, Z.; Kong, J.; Fu, G. Silica nanoparticle supported molecularly imprinted polymer layers with varied degrees of crosslinking for lysozyme recognition. *Anal. Chim. Acta* **2013**, *779*, 82–89. [CrossRef]
16. Jin, Y.; Jiang, M.; Shi, Y.; Lin, Y.; Peng, Y.; Dai, K.; Lu, B. Narrowly dispersed molecularly imprinted microspheres prepared by a modified precipitation polymerization method. *Anal. Chim. Acta* **2008**, *612*, 105–113. [CrossRef] [PubMed]
17. Feng, Q.-Z.; Zhao, L.-X.; Yan, W.; Lin, J.-M.; Zheng, Z.-X. Molecularly imprinted solid-phase extraction combined with high performance liquid chromatography for analysis of phenolic compounds from environmental water samples. *J. Hazard. Mater.* **2009**, *167*, 282–288. [CrossRef] [PubMed]
18. Huang, C.Y.; Syu, M.J.; Chang, Y.S.; Chang, C.H.; Chou, T.C.; Liu, B.D. A portable potentiostat for the bilirubin-specific sensor prepared from molecular imprinting. *Biosens. Bioelectron.* **2007**, *22*, 1694–1699. [CrossRef]
19. Urraca, J.L.; Moreno-Bondi, M.C.; Orellana, G.; Sellergren, B.; Hall, A.J. Molecularly Imprinted Polymers as Antibody Mimics in Automated On-Line Fluorescent Competitive Assays. *Anal. Chem.* **2007**, *79*, 4915–4923. [CrossRef]
20. Shen, X.; Zhu, L.; Liu, G.; Yu, H.; Tang, H. Enhanced Photocatalytic Degradation and Selective Removal of Nitrophenols by Using Surface Molecular Imprinted Titania. *Environ. Sci. Technol.* **2008**, *42*, 1687–1692. [CrossRef]
21. Hu, Y.; Liu, R.; Zhang, Y.; Li, G. Improvement of extraction capability of magnetic molecularly imprinted polymer beads in aqueous media via dual-phase solvent system. *Talanta* **2009**, *79*, 576–582. [CrossRef]
22. Li, Y.; Li, X.; Dong, C.; Qi, J.; Han, X. A graphene oxide-based molecularly imprinted polymer platform for detecting endocrine disrupting chemicals. *Carbon* **2010**, *48*, 3427–3433. [CrossRef]
23. Li, Q.; Yang, K.; Liang, Y.; Jiang, B.; Liu, J.; Zhang, L.; Liang, Z.; Zhang, Y. Surface Protein Imprinted Core–Shell Particles for High Selective Lysozyme Recognition Prepared by Reversible Addition–Fragmentation Chain Transfer Strategy. *ACS Appl. Mater. Interfaces* **2014**, *6*, 21954–21960. [CrossRef]
24. Blake, C.C.F.; Koenig, D.F.; Mair, G.A.; North, A.C.T.; Phillips, D.C.; Sarma, V.R. Structure of hen egg-white lysozyme: A three-dimensional Fourier synthesis at 2 Å resolution. *Nature* **1965**, *206*, 757–761. [CrossRef]
25. Held, J.; van Smaalen, S. The active site of hen egg-white lysozyme: Flexibility and chemical bonding. *Acta Crystallogr. D Biol. Crystallogr.* **2014**, *70*, 1136–1146. [CrossRef] [PubMed]
26. Carrillo, W.; García-Ruiz, A.; Recio, I.; Moreno-Arribas, M.V. Antibacterial Activity of Hen Egg White Lysozyme Modified by Heat and Enzymatic Treatments against Oenological Lactic Acid Bacteria and Acetic Acid Bacteria. *J. Food Prot.* **2014**, *77*, 1732–1739. [CrossRef]
27. Vilcacundo, R.; Méndez, P.; Reyes, W.; Romero, H.; Pinto, A.; Carrillo, W. Antibacterial Activity of Hen Egg White Lysozyme Denatured by Thermal and Chemical Treatments. *Sci. Pharm.* **2018**, *86*, 48. [CrossRef]
28. Available online: <https://www.sigmaaldrich.com/DE/en/sds/sigma/l6876> (accessed on 23 November 2021).
29. Shih, Y.-C.; Prausnitz, J.M.; Blanch, H.W. Some characteristics of protein precipitation by salts. *Biotechnol. Bioeng.* **1992**, *40*, 1155–1164. [CrossRef]
30. Habel, J.; Chapman, P.; Choudhary, G. From Optimization to Automation: Multidimensional (Multi-D) Histidine-Tag Protein Purification, Ver C. *BioRad Technol. Bull.* **2016**, 6725.
31. Elms, P.; Choudhary, G.; Habel, J. Automated mAb Workflows: Combining Multidimensional (Multi-D) Purifications with Product Analysis, Ver C. *BioRad Laboratories. Bull.* **2015**, *15*, 0116.